Journal of Catalysis 258 (2008) 265–272

Contents lists available at ScienceDirect

Journal of Catalysis

www.elsevier.com/locate/jcat

Enhancement of catalytic performance by creating shell layers on sulfonic acid-functionalized monodispersed mesoporous silica spheres

Tomiko M. Suzuki *, Tadashi Nakamura, Eiichi Sudo, Yusuke Akimoto, Kazuhisa Yano *

Toyota Central Research and Development Labs. Inc., Nagakute, Aichi 480-1192, Japan

ARTICLE INFO

Article history:
Received 18 April 2008
Revised 10 June 2008
Accepted 16 June 2008
Available online 16 July 2008

Keywords:
Mesoporous silica
Monodispersed spheres
Core–shell structure
Sulfonic acid-functionalized
Acid catalyst

ABSTRACT

New types of organically functionalized core/shell monodispersed mesoporous silica spheres (MMSS) containing catalytic sites (sulfonic acid groups) in the core portion and adsorption sites (hydrophobic organic functional groups) in the shell portion were successfully synthesized by the co-condensation/expansion method. These SO_3H-core/hydrophobic-shell MMSS have radially aligned hexagonal mesopores and display different chemical properties in the core and shell portions. The acid catalytic activities of the SO_3H-core/hydrophobic-shell MMSS were studied in condensation reactions between 2-methylfuran and acetone. It was found that the catalytic activities were most enhanced by incorporating ethyl or propyl groups into the shell portion. These groups have molecular sizes and affinity that are particularly suitable for entry of two reactants with completely different polarity at a proper balance and discharge of products. In addition, the SO_3H-core/hydrophobic-shell MMSS had higher catalytic activities than MMSS having randomly distributed SO_3H and hydrophobic groups.

1. Introduction

In recent years, a variety of mesoporous silicas have been studied towards the goal of applying them in fields such as catalysis, adsorption, separation, ion exchange and sensor design. The principal advantages of these materials are their uniform mesopores, high specific surface areas and high concentrations of surface hydroxyl groups.

The syntheses of organic–inorganic hybrid mesoporous silicas that incorporate organic functional groups into their mesopores have been conducted with the aim of utilizing these materials as novel heterogeneous catalysts [1,2]. In general, heterogeneous catalysts have advantages in terms of separation and regeneration from reaction solutions.

Mesoporous silicas that have been functionalized by sulfonic acid groups have attracted much attention as alternatives to traditional homogeneous acid catalysts such as sulfuric acid, fluoric acid, and organic sulfonic acids [1,3]. For example, propylsulfonic acids have been incorporated into mesoporous silicas such as MCM, FSM, and SBA in order to investigate acid catalysis reactions. High catalytic activities for condensation and addition reactions [4–10] and esterification reactions [11,12] have been reported. In addition, other acidic arenesulfonic acids [12–17] and perfluorosulfonic acids [18–20] have been incorporated into mesoporous silicas for higher catalytic activity.

It is expected that the incorporation of hydrophobic moieties into mesopores would lead to the enhancement of catalytic performance due to changes in the adsorption and diffusion of reactants, products, and intermediate species. There have been some reports on the syntheses of organically functionalized mesoporous silicas containing sulfonic acid groups and other organic moieties in order to control the hydrophobic character of the mesopore surfaces. Margolese et al. synthesized SBA-15 that incorporated benzyl or methyl groups as the second organic functional group using co-condensation, and confirmed that sulfonic acid and the second organic functional group were incorporated into the silica skeleton by ^{13}C CP MAS NMR analysis [21]. Díaz et al. succeeded in the synthesis of alkyl (methyl or propyl) and propylsulfonic acid functionalized MCM-41 [22]. In evaluating the esterification reaction of glycerol with lauric and oleic acids using the organically functionalized MCM-41, it was found that the conversion of lauric acid and the selectivity for monoglyceride was improved by the incorporation of methyl groups [23,24].

We have previously reported that monodispersed mesoporous silica spheres (MMSS) possessing highly ordered hexagonal fine mesopores can be obtained by reacting tetramethoxysilane (TMOS) and *n*-alkyltrimethylammonium halide (C_nTMAX, $X = Cl$, Br) [25–27]. We studied the effects of pore size on base catalysis using amino-functionalized MMSS by a grafting method. It was found that the reaction mostly proceeded inside the radially aligned mesopores (effectiveness factor: 0.63) and that the optimum pore size for the amino-functionalized MMSS was affected by changing

* Corresponding authors. Fax: +81 561 63 6507.
E-mail addresses: tomiko@mosk.tytlabs.co.jp (T.M. Suzuki), k-yano@mosk.tytlabs.co.jp (K. Yano).

0021-9517/$ – see front matter
doi:10.1016/j.jcat.2008.06.021

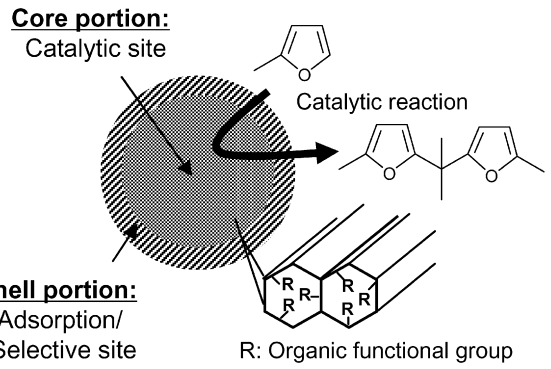

Fig. 1. Structure of new core/shell type catalyst based on monodispersed mesoporous silica spheres.

the type and size of the substituent groups on the reactants [28]. We also synthesized amino or sulfonic acid-functionalized MMSS by co-condensation. The catalytic activities of these MMSS were higher than other types of mesoporous catalysts, and the radially aligned mesopores in MMSS were found to be very advantageous in terms of allowing entry by reactants and discharge of reaction products [29,30]. In addition, we recently synthesized core/shell MMSS that had a hydrophilic core and a hydrophobic shell. It was prepared by adding a TMOS/propyltrimethoxysilane mixture to the product obtained after the reaction with TMOS was complete (expansion method) [31,32]. The radial alignment of the hexagonal mesopores was retained in the expanded particles.

One of the challenges in utilizing core/shell structures is to create a novel catalyst consisting of a catalytic core and a functionalized shell that exhibits affinity to the appropriate reactants. We therefore attempted to synthesize core/shell MMSS consisting of a catalytic active site (sulfonic acid) in the core portion and an adsorption site (hydrophobic organic groups) in the shell portion by the co-condensation/expansion method (Fig. 1). The mixtures of TMOS and mercaptopropyltrimethoxysilane or alkyltrimethoxysilane were used as the silica precursors for the core and the shell portions, respectively. The mercapto group was subsequently oxidized into a sulfonic acid group. Consequently, we have succeeded for the first time in obtaining organically separately-functionalized core/shell MMSS with a radially aligned pore structure by the co-condensation/expansion method. It was found that the catalytic activities of the MMSS were influenced by the type and thickness of the shell portion, and the core/shell MMSS had higher catalytic activities than equivalent MMSS having randomly distributed catalytic active sites (sulfonic acid) and adsorption sites (hydrophobic organic groups).

2. Experimental

2.1. Chemicals and catalyst synthesis

3-Mercaptopropyltrimethoxysilane (MPTMS), methyltrimethoxysilane (MeTMS), ethyltrimethoxysilane (EtTMS), propyltrimethoxysilane (PrTMS), isobutyltrimethoxysilane (iBuTMS), and phenyltrimethoxysilane (PhTMS) were purchased from Aldrich. Hexadecyltrimethylammonium chloride (C_{16}TMACl) and TMOS were purchased from Tokyo Kasei. 1 M sodium hydroxide solution, methanol, hydrochloric acid, hydrogen peroxide (30%), 2-methylfuran, and acetone were purchased from Wako Inc. All chemicals were used as received without further purification.

Core/shell MMSS samples were obtained by co-condensation and subsequent expansion reactions, in which a silica precursor of a type different from the initial one was added to a solution containing particles of the material [31,32].

The synthesized materials are abbreviated as MS-X/Y, where MS denotes the mesoporous silica and X denotes the type of organic functional group in the core portion, e.g., SH (precursor: mercaptopropyl) or SO_3H (sulfonic acid). Y denotes the type of organic functional group in the shell portion: Me (methyl group), Et (ethyl group), Pr (propyl group), iBu (isobutyl group), Ph (phenyl group), TMOS (no organic group). The molar fraction of organic trimethoxysilane in the co-condensation was 10 mol%, and the amount of silica source used for the shell portion was usually half of that used for the core portion in a typical synthesis. When the amount of additive silica source for the shell portion was double the amount of the core portion, *2 signs are added to the sample names. In case of MS-SO_3H/Y with different molar fraction of organic trimethoxysilane in the shell portion, we abbreviate the synthesized materials as MS-SO_3H/YZ. Z denotes the molar fraction of organic trimethoxysilane (5, 20, 30, 40%).

A typical preparation of MS-SO_3H/Me is as follows. 7.04 g of C_{16}TMACl and 6.84 g of 1 M sodium hydroxide solution were dissolved in 1600 g of a methanol/water (49/51 w/w) solution. 34.7 mmol of a TMOS/MPTMS (90/10 mol/mol) mixture was added to the solution with vigorous stirring at 298 K. After the addition of the TMOS/MPTMS mixture, the clear solution suddenly turned opaque and a white precipitate formed. Next, 3.42 g of 1 M sodium hydroxide solution and half the molar amount of TMOS/MeTMS (90/10 mol/mol, 17.35 mmol) mixture were added to the solution after a period of 30 min. After 8 h of continuous stirring, the mixture was aged overnight without stirring at room temperature. The resulting white powder was then filtered and washed three times with distilled water and dried at 318 K for 72 h. The powder (1 g) was refluxed in 100 mL of ethanol containing 1 mL of hydrochloric acid at 333 K for 3 h to remove the templates. The powder was filtered, washed several times with ethanol and dried at 318 K. The SH groups were converted into SO_3H groups by mild oxidation with H_2O_2 [30]. In the oxidation step, the mixture consisting of 0.7 g of MS-SH/Me and 10 ml of H_2O_2 (30%) was heated at 323 K for 3 h with constant stirring.

2.2. Characterization

Powder X-ray diffraction measurements were carried out on a Rigaku Rint-2200 X-ray diffractometer using Cu$K\alpha$ radiation. Scanning electron micrographs (SEMs) were obtained with a SIGMA-V (Akashi Seisakusho). The sample surfaces were coated with gold before the measurements. The diameters of 50 particles in a typical SEM picture were measured to determine an average particle diameter. The particle diameter distribution was judged from the standard deviation. The nitrogen adsorption isotherm was measured using a Belsorp-mini II (BEL Japan) at 77 K. The sample was evacuated at 373 K under less than 10^{-3} mm Hg before measurement. The pore diameter was calculated by the Barrett–Joyner–Halenda (BJH) method. By considering the linearity of a Brunauer–Emmett–Teller (BET) plot, the specific surface area was calculated using adsorption data in the P/P_0 range from 0.05 to 0.13. Transmission electron micrographs were obtained with a Jeol-200CX TEM at an acceleration voltage of 200 kV. ^{29}Si magic-angle-spinning (MAS) nuclear magnetic resonance (NMR) and ^{13}C cross-polarization (CP) NMR analyses were carried out on a Bruker AVANCE 400 spectrometer at 79.49 MHz for ^{29}Si and 100.61 MHz for ^{13}C. The ^{29}Si MAS NMR spectra were measured with a 60 s repetition delay and 3 μs pulse width. The ^{13}C CP MAS NMR spectra were measured with a 2 s repetition delay, 2 ms contact time, and a 2.8 μs ^{1}H 90° pulse. The ^{29}Si and ^{13}C chemical shifts were referenced to tetramethylsilane and glycine, respectively. For both measurements, the spinning rate was 5 kHz. Raman spectra were measured with a JASCO micro-Raman system NRS-3300 spectrometer using the 532 nm laser line. The system was equipped with

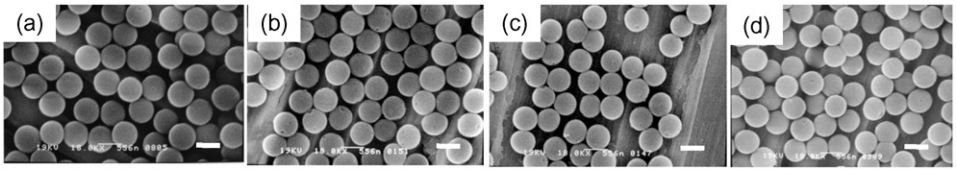

Fig. 2. Scanning electron micrographs of (a) MS-SO_3H/TMOS, (b) MS-SO_3H/Et, (c) MS-SO_3H/Pr, and (d) MS-SO_3H/iBu. Scale bar represents 0.56 μm.

Table 1
Properties of SO_3H-core/hydrophobic-shell MMSS

Sample	Core/shell ratio[a]	Average particle diameter (nm)	Standard deviation (%)	XRD		Nitrogen adsorption			Acidity (mmol H^+/g)
				d_{100} (nm)	Intensity (cps)	Pore size (nm)	Specific surface area (m^2/g)	Pore volume (ml/g)	
MS-SO_3H/TMOS	2	580	5.5	3.4	11,000	2.0	1260	0.71	0.66
MS-SO_3H/Me	2	560	8.0	3.4	9800	2.0	1130	0.70	0.67
MS-SO_3H/Et	2	570	5.8	3.4	10,500	2.0 (2.0)[b]	1140 (1050)	0.65 (0.62)	0.63
MS-SO_3H/Pr	2	580	5.6	3.5	10,300	2.0	1170	0.67	0.63
MS-SO_3H/iBu	2	590	7.5	3.3	7800	1.8	1020	0.50	0.62
MS-SO_3H/Ph	2	580	5.0	3.4	10,600	1.7	1040	0.52	0.64
MS-SO_3H/Pr*2	0.5	710	4.5	3.4	11,200	1.9	1130	0.61	0.41
MS-SO_3H-Et	–	570	6.0	3.4	13,000	2.0	1100	0.62	0.61
MS-SO_3H-Pr	–	530	7.6	3.4	9600	1.8	1040	0.53	0.64
MS-SO_3H	–	500	6.5	3.4	11,600	2.0	1050	0.62	0.72
MS-Et	–	620	5.4	3.5	11,800	2.2	1160	0.81	–

[a] Si molar ratio of core to shell portion.
[b] In parentheses: The pretreatment of the sample was carried out at 323 K (the same temperature of the catalyst preparation).

a holographic notch filter, a 600 grooves/mm holographic grafter, a 100× microscope objective, and a Peltier-cooled (−330 K) CCD detector. Elemental analysis for S was conducted by the flask combustion method and ion chromatography. CH elemental analyses were carried out on an Elementer varioEL elemental analyzer. The acid-exchange capacity was determined by titration with NaOH. In a typical procedure, 50 mg of sample was suspended in 50 mL of a 10 wt% aqueous NaCl solution. The resulting suspension was stirred at room temperature for 18 h until equilibrium was reached and then titrated by drop wise addition of a 0.05 M NaOH solution.

2.3. Catalytic reactions

The liquid-phase condensation of 2-methylfuran (MF) with acetone to form 2,2-bis(5-methylfuryl)propane (DMP) was typically carried out as follows. All catalysts were dried in a vacuum at 323 K for 1 h prior to the reaction.

A reaction mixture consisting of 60 mg of the mesoporous silica catalyst and 0.6 g of 2-methylfuran in 1.1 g of acetone was heated at 323 K for 8 h with constant stirring. The mixture was filtered and the solids were washed with fresh solvent. The filtrate and cleaning fluid were combined and analyzed using a gas chromatograph (Shimadzu, GC-2014) with a 30 m capillary column of DB-5.

2.4. Adsorption test

The adsorption of MF on the MMSS was studied as follows.

A solution consisting of 20 mg of MMSS and 0.3 g of MF in 1.1 g of acetone (or methanol) was stirred at 273 K (or 323 K) for 10 min. The solution was filtered, and the filtrate was analyzed using a gas chromatograph.

3. Results and discussion

3.1. Synthesis of core/shell MMSS

3.1.1. Morphologies and physical properties of core/shell MMSS

Organically functionalized core/shell MMSS samples containing mercaptopropyl groups in the core portions and hydrophobic organic groups in the shell portions (SH-core/hydrophobic-shell MMSS) were synthesized by the addition of different silica precursors to the original MMSS (co-condensation/expansion method). Five types of hydrophobic organic functional groups were used for the components of the shell portions: methyl (Me), ethyl (Et), propyl (Pr), isobutyl (iBu), and phenyl (Ph) groups. The molar fraction of organic trimethoxysilane was 10 mol% and the amount of additive silica source for the shell portion was half the amount of the core portion. The mercaptopropyl groups in the core portion were then oxidized into sulfonic acid groups, resulting in the production of sulfonic acid-core/hydrophobic-shell MMSS (SO_3H-core/hydrophobic-shell MMSS). From SEM observations, it was clear that the particle diameters and the monodispersity of the SH-core/hydrophobic-shell MMSS remained unchanged after oxidation. SEM images of the SO_3H/hydrophobic-shell MMSS samples are shown in Fig. 2. Table 1 summarizes the properties of the samples. Particles with a standard deviation below 10% were considered to be monodispersed. All synthesized samples were monodispersed spherical particles. The average particle diameters of the samples substantially increased upon addition of the shell layers (560–590 nm) when compared to the diameter of the original MS-SO_3H (500 nm). This result indicates that the additive silica sources preferred to react with the silanol groups on the surface of the existing particles rather than generating new particles by reactions between the silica sources.

The degree of mesostructural ordering in the core/shell MMSS samples was evaluated by powder XRD analysis. Fig. 3 shows the XRD patterns of the core/shell MMSS samples and Table 1 summarizes the values and intensities of d_{100} in the XRD patterns. The patterns had three peaks indexed to the d_{100}, d_{110}, and d_{200} diffractions, indicating that the mesopores in all the samples were highly ordered. The degree of mesostructural ordering in the SO_3H-core/hydrophobic-shell MMSS samples was equivalent to that of the precursor SH-core/hydrophobic-shell MMSS samples.

The nitrogen adsorption–desorption isotherms were then measured and the pore-size distributions were analyzed by the BJH method. Fig. 4 shows the isotherms and the pore size distributions for MS-SO_3H/TMOS and MS-SO_3H/Et. Pore sizes, specific surface areas, and pore volumes of the samples are also summarized in Ta-

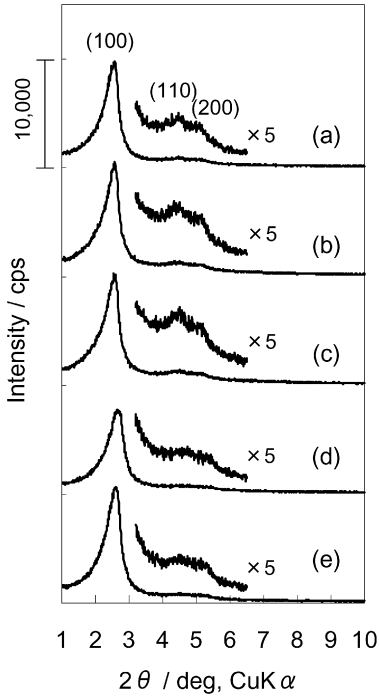

Fig. 3. XRD spectra of the samples: (a) MS-SO_3H/Me, (b) MS-SO_3H/Et, (c) MS-SO_3H/Pr, (d) MS-SO_3H/iBu, and (e) MS-SO_3H/Ph.

ble 1. Before the nitrogen adsorption measurements, the samples were pretreated in a vacuum at 373 K to remove water. However, the catalyst preparation was conducted at 323 K. Then, the nitrogen adsorption isotherm of MS-SO_3H/Et was obtained by pretreating the sample at 323 K. It was confirmed that physisorption property of MS-SO_3H/Et hardly changed by changing the pretreating temperature (parentheses in Table 1). The isotherms of the SO_3H-core/hydrophobic-shell are "type IV," and all of the samples that were obtained showed the same "type IV" pattern. When the molecular size of the hydrophobic groups that were incorporated into the shell portion increased, pore volumes decreased considerably due to the incorporation of bulky organic groups inside the mesopores.

3.1.2. Chemical properties of core/shell MMSS

The sulfonic acid group was identified by Raman spectroscopy [30,33]. Fig. 5 shows the spectra of MS-SO_3H/Et and MS-SO_3H/Ph. Bands originating from the methylene group (2930 and 1450 cm^{-1}) were clearly observed, while the band from the mercapto group (2580 cm^{-1}) had disappeared and new bands from the sulfonic acid group appeared, SO_3 (1027 cm^{-1}) and C–S (817 cm^{-1}), in the spectrum of MS-SO_3H/Et (a). This indicates that the mercapto groups in SH-functionalized MMSS were converted to sulfonic acid groups by the oxidation process. In the spectrum of MS-SO_3H/Ph (b), the bands from the propylsulfonic acid in the core portion and the phenyl group (3059, 1595, 999 cm^{-1}) in the shell portion were observed, and it was clear that the hydrophobic group in the shell remained unchanged after oxidation. Similar results were observed for all of the SO_3H-core/hydrophobic-shell MMSS samples.

Fig. 6 shows the ^{29}Si MAS NMR spectrum of MS-SO_3H/Pr. Three clear resonance peaks derived from Q^n [$Q^n = Si(OSi)_n(OH)_{4-n}$, $n = 2$–4, Q^4: $\delta = -110$ ppm, Q^3: $\delta = -100$ ppm, Q^2: $\delta = -90$ ppm] and two peaks derived from T^m [$T^m = RSi(OSi)_m(OH)_{3-m}$, $m = 1$–3, T^3: $\delta = -65$ ppm, T^2: $\delta = -55$ ppm] were observed. The presence of the T^m peak indicates the incorporation of an organic functional moiety into the silica skeleton. This confirmed that the organic functional group remained in the silica skeleton after oxidation.

Fig. 7 shows the results of the ^{13}C CP MAS NMR analysis. The spectrum of MS-SO_3H/Pr (a) exhibited peaks derived from the C atoms of the propylsulfonic groups ($\delta = 11$, 21, 53 ppm) [30] in

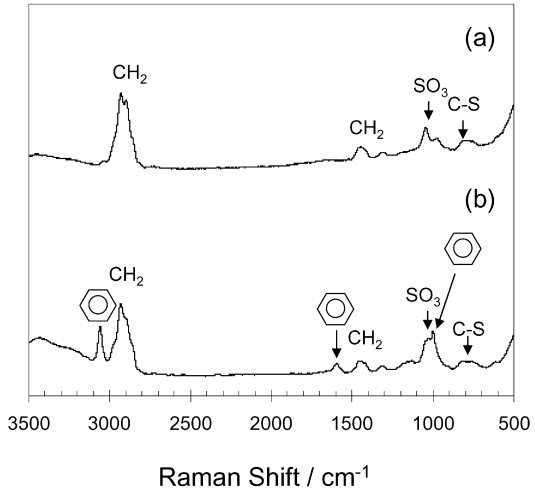

Fig. 5. Raman spectra of (a) MS-SO_3H/Et and (b) MS-SO_3H/Ph.

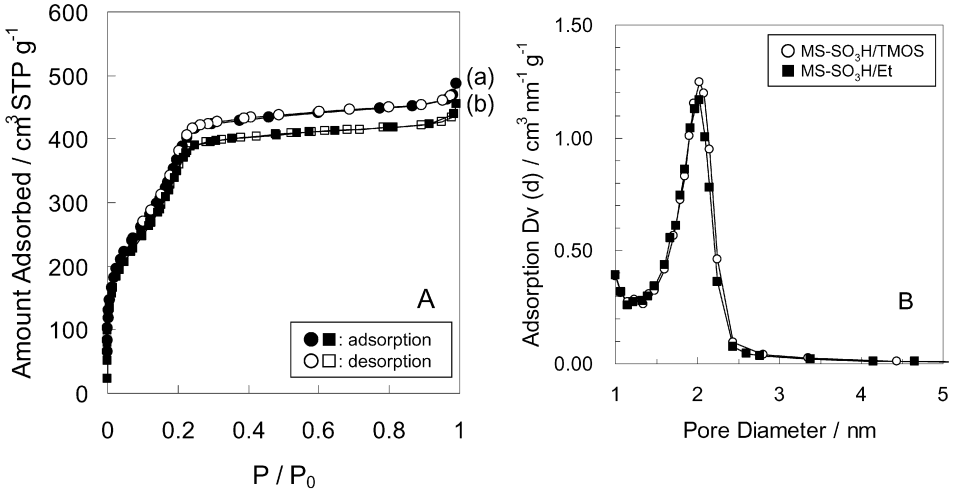

Fig. 4. (A) Nitrogen adsorption–desorption isotherms and (B) pore size distributions of (a) MS-SO_3H/TMOS and (b) MS-SO_3H/Et.

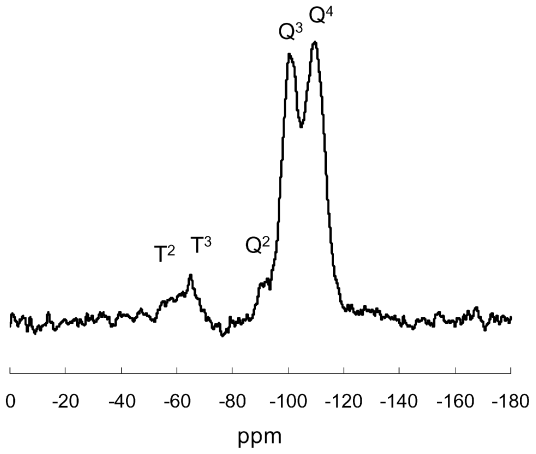

Fig. 6. ^{29}Si MAS NMR spectrum of MS-SO_3H/Pr.

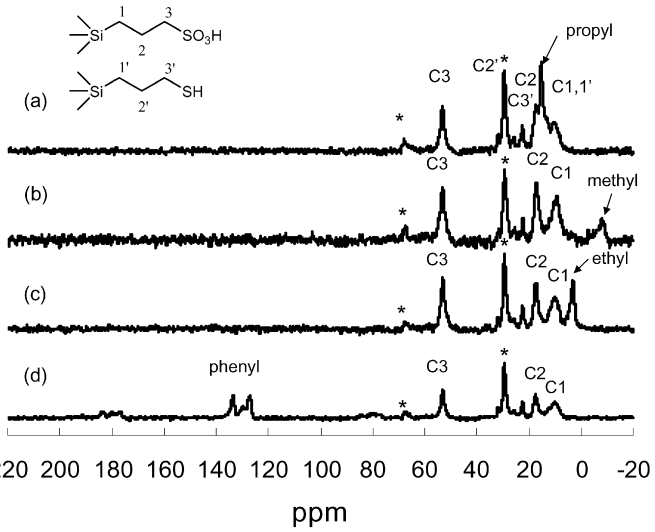

Fig. 7. ^{13}C CP MAS NMR spectra of (a) MS-SO_3H/Pr, (b) MS-SO_3H/Me, (c) MS-SO_3H/Et, and (d) MS-SO_3H/Ph. *: Signals of residual surfactant (C_{16}TMACl) carbons.

the core portion and the propyl groups ($\delta = 16$ ppm) in the shell portion. Although the alkyl groups in the core and shell portions were difficult to distinguish in the Raman spectrum due to the overlap of the two bands, each of the alkyl groups were distinguishable in the NMR spectrum. Small peaks from an un-oxidized mercaptopropyl group (C1′, C3′, C2′: $\delta = 11$, 23, 29 ppm) [30] were also observed, indicating that some of the SH groups could not be oxidized. Peaks from the surfactant used for the template were also observed (Fig. 7, *) [30], and the peak from the methylene group of the surfactant was overlapped with the peak from the mercaptopropyl group (C2′). Similar results were obtained for MS-SO_3H/Me (b), MS-SO_3H/Et (c) and MS-SO_3H/Ph (d) samples in which another hydrophobic group was incorporated in the shell portion.

The acidities (the number of H^+ per unit) of the core/shell MMSS samples were determined by titration, and the results are listed in Table 1. The amount of H^+ in MMSS that was not organically-functionalized was 0.36 mmol H^+/g, due to silanol groups inside the mesopores. Therefore, this value was deducted from the acidity measured in the experiment [30]. Consequently, the acidity of the core/shell MMSS was in the range between 0.62 and 0.67 mmol H^+/g. This confirmed that sulfonic acid groups were successfully incorporated into the SO_3H-core/hydrophobic-shell MMSS samples.

Table 2
Results of elemental analysis for SO_3H-core/hydrophobic-shell MMSS

Sample	Elemental analysis (wt%)			C/S atomic ratio
	C	H	S	
MS-SO_3H/TMOS	5.5	3.1	2.1	7.0
MS-SO_3H/Me	4.4	3.2	2.0	5.9
MS-SO_3H/Et	5.5	2.9	2.2	7.0
MS-SO_3H/Pr	6.5	3.1	2.1	8.3
MS-SO_3H/iBu	6.9	3.2	2.2	8.4
MS-SO_3H/Ph	8.1	3.2	2.1	10.3
MS-SO_3H	5.1	3.8	2.1	6.5

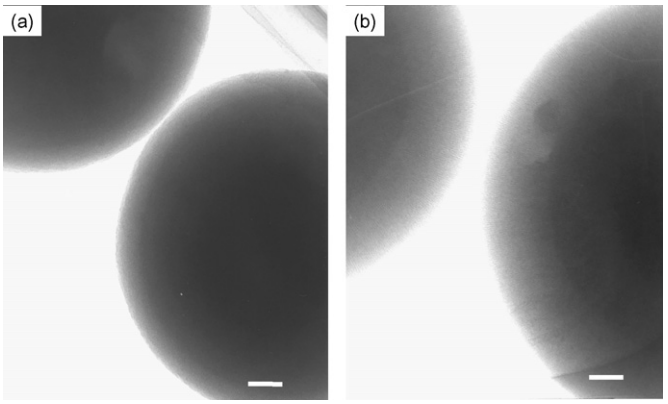

Fig. 8. Transmission electron micrographs of gold incorporated (a) MS-SH/Pr and (b) MS-SH/Pr*2. Scale bar represents 50 nm.

Next, elemental analyses of SO_3H-core/hydrophobic-shell MMSS samples were conducted. These results are shown in Table 2 along with the C/S atomic ratios of the samples. The S contents of the SO_3H-core/hydrophobic-shell MMSS were 2 to 2.2 wt% (0.62–0.69 mmol g^{-1}), and it was confirmed that almost the same amount of S was incorporated into all MMSS samples. These values were in agreement with the acidity calculated from the titration results. The C/S ratios increased with increasing number of carbon atoms in the hydrophobic group of the shell portion, as expected. Although the theoretical C/S values for MS-SO_3H/TMOS and MS-SO_3H were both 3, the C/S ratios that were determined experimentally were 7.0 and 6.5, respectively, more than twice the theoretical values. The presence of the residual "non-extracted" surfactants that were detected by the NMR measurements and the portions of the sulfur eliminated from the functionalized silica during the oxidation process might bring about these differences.

3.1.3. Structures of core/shell MMSS

TEM observations were performed in order to confirm the internal structures and mesopore arrangements in the core/shell MMSS. SH-core/hydrophobic-shell MMSS samples were used as specimens, taking advantage of the specific adsorption of gold ions to the mercapto group. The samples were immersed in a solution containing gold ions and then reduced chemically using formaldehyde. Fig. 8 shows TEM images of MS-SH/Pr and MS-SH/Pr*2 samples. The amount of additive silica source in MS-SH/Pr was half amount of the core portion, and that was doubled in MS-SH/Pr*2. An ovoid structure can clearly be seen in Fig. 8, indicating gold (dark part) was selectively adsorbed to the core portion. The thickness of the shell was proportional to the amount of the additive silica source that was used. The thicknesses of the shells of MS-SH/Pr and MS-SH/Pr*2 were estimated to be 35 and 110 nm, respectively. These values agreed with the calculated values, which assume a proportional distribution based on the average particle diameter derived from SEM images. In addition, Fig. 9 shows a TEM image of calcined MS-SO_3H/Et. Removing the organic components in MMSS by

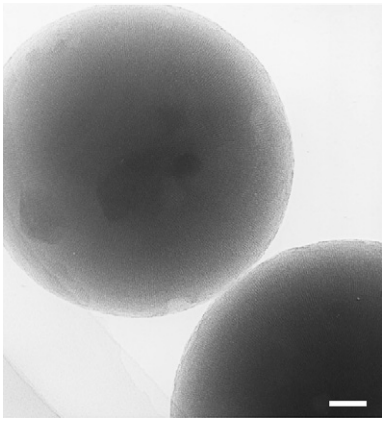

Fig. 9. Transmission electron micrograph of calcined MS-SO_3H/Et. Scale bar represents 50 nm.

Table 3
Results of the condensation reaction of 2-methylfuran (**1**) and acetone (**2**) for 2 h[a]

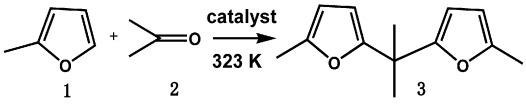

Entry	Catalyst	Yield (%)
1	MS-SO_3H/TMOS	56
2	MS-SO_3H/Me	57
3	MS-SO_3H/Et	69
4	MS-SO_3H/Pr	72
5	MS-SO_3H/iBu	64
6	MS-SO_3H/Ph	54
7	MS-SO_3H	58
8	MS-SO_3H-Et	62
9	MS-SO_3H-Pr	63
10	MS-SH/Et	1
11	MS-Et	0
12	MMSS	0

[a] Reaction conditions: 60 mg MMSS samples, 0.3 g 2-methylfuran, 1.1 g acetone, 323 K, 2 h. Yields determined by gas chromatograph.

calcining [30], clear TEM image could be obtained for the center portion of the particles. The hexagonal mesopores were arrayed in a radial pattern from the center towards the outside of the spheres, as was observed in the expanded-MMSS [32]. From these results, it was clear that organically functionalized core/shell MMSS that incorporated sulfonic acid in the core portion and hydrophobic groups in the shell portion had been successfully synthesized by the co-condensation/expansion method for the first time.

3.2. Acid catalytic activity of core/shell MMSS

The effect of the shell layer on the acid catalytic activities of MMSS was studied using SO_3H-core/hydrophobic-shell MMSS samples. In a typical strong acid-catalyzed condensation reaction (as depicted in Table 3), 2,2-bis(5-methylfuryl)propane (DMP, **3**) is produced from 2-methylfuran (MF, **1**) and acetone (**2**). Bisfurylalkanes are important intermediates in macromolecular chemistry; therefore these reactions are used to evaluate the catalytic performance of solid sulfonic acids [4,19]. The type of hydrophobic group in the shell was changed in the SO_3H-core/hydrophobic-shell MMSS samples in order to understand how the shell layer affects the catalytic activity. Table 3 shows the results for the acid catalytic reactions. Two or three runs were performed for all the reaction and yield values listed in the table were reproducible (within 2% error). MMSS (no organic functional groups), MS-Et (containing only ethyl groups), and MS-SH/Et (precursor of SO_3H-core/ethyl group-shell MMSS) showed almost no catalytic activity (Entries 12, 11, 10) due to the absence of SO_3H groups. The yield of DMP using MS-SO_3H, which was SO_3H-functionalized MMSS without a shell, was 58% (Entry 7). When MS-SO_3H was covered by a shell with an inorganic component, the yield decreased slightly to 56% (Entry 1: MS-SO_3H/TMOS). It is assumed that the reaction was slightly suppressed by the introduction of the shell layer because the catalytic sites were in the core portions of the spheres. The shell layer could suppress diffusion of the reactants and products. However, the incorporation of ethyl, propyl, and isobutyl groups into the shell layer led to increase in the yield (Entries 3–5). In particular, the yields were drastically increased to 69 or 72% (Entries 3, 4) by the incorporation of ethyl or propyl groups. The incorporation of methyl or phenyl groups led to only minor changes in the yield (Entries 2, 6) compared to MS-SO_3H/TMOS. Fig. 10 shows the catalytic activities of various SO_3H-core/hydrophobic-shell MMSS. MS-SO_3H/Et and MS-SO_3H/Pr exhibited excellent catalytic activity through the reaction; the yield at 2 h for these catalyst were about 1.2–1.3 times higher than that for MS-SO_3H/TMOS. MF (one of the reactants) and DMP (product) are hydrophobic, but acetone (the other reactant) is hydrophilic. In addition, the molecular size of the product is larger than that of the reactant. Therefore, an effective catalyst must have mesopores that display well-balanced affinity against reactants and suitable pore sizes for easy transfer of the reactants and product. The above results suggest that the incorporation of ethyl or propyl groups in the shell portion satisfied the demand for an effective catalyst. Moreover, by incorporating hydrophobic groups into the shell layer, the water generated as a by product during the reaction is easily removed from the particles, resulting in further enhancement of the acid catalytic reaction.

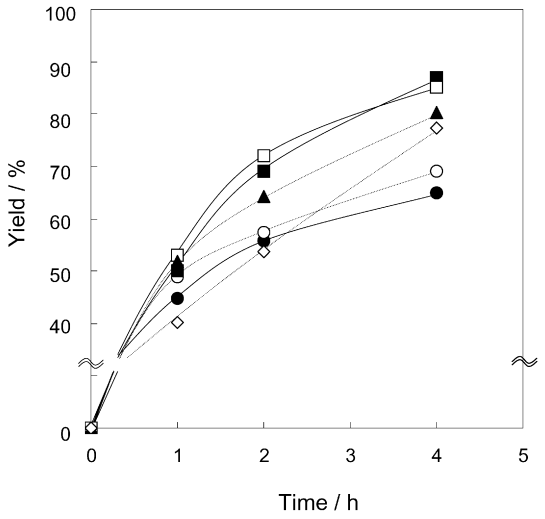

Fig. 10. Changes in the activity of MS-SO_3H/shell catalysts in condensation reaction of 2-methylfuran and acetone: (●) MS-SO_3H/TMOS, (○) MS-SO_3H/Me, (■) MS-SO_3H/Et, (□) MS-SO_3H/Pr, (▲) MS-SO_3H/iBu, (◇) MS-SO_3H/Ph.

Inumaru et al. studied the molecular selective adsorption of nonylphenol to alkyl group-functionalized mesoporous silica (MPS) in aqueous solution. They reported that octyl group-functionalized MPS adsorbed much more nonylphenol than dodecyl group-functionalized MPS. The reason for the difference in the adsorption is that the hydrophobicity of the dodecyl group is too strong to adsorb nonylphenol while the moderate hydrophobicity of the octyl group is suitable for the effective adsorption of nonylphenol [34]. Then, tests were conducted to study the adsorption efficiency of the reactant (MF) to the SO_3H-core/hydrophobic-shell MMSS samples. The outcomes are shown in Table 4. Two or three runs were performed and the residual amounts of MF listed in the table were reproducible (within 1% error). Because the reaction proceeds

Table 4
Results of adsorption of 2-methylfuran (MF) on various SO_3H-core/hydrophobic-shell MMSS

MMSS	Residual amount of MF (%)	
	Solvent: acetone[a] (273 K)	Solvent: methanol[b] (323 K)
MS-SO_3H/TMOS	88 (1)[c]	88 (0)[c]
MS-SO_3H/Me	88 (2)	86 (0)
MS-SO_3H/Et	81 (3)	81 (0)
MS-SO_3H/Pr	83 (2)	84 (0)
MS-SO_3H/iBu	84 (1)	84 (0)
MS-SO_3H/Ph	91 (2)	90 (0)
MS-SO_3H-Et	87 (1)	85 (0)

[a] Adsorption conditions: 20 mg MMSS samples, 0.3 g 2-methylfuran, 1.1 g acetone, 273 K, 10 min.
[b] Adsorption conditions: 20 mg MMSS samples, 0.3 g 2-methylfuran, 1.1 g methanol, 323 K, 10 min.
[c] Yield (%) of 2,2-bis(5-methylfuryl)propane (DMP).

quickly at 323 K, the absorption tests were performed at 273 K in the presence of acetone and the concentrations of residual MF were measured. In the case of MS-SO_3H/TMOS, which contained no organic functional groups in the shell portion, the concentration of the residual MF was 88%. This value decreased (81, 83, or 84%) when MS-SO_3H/Et, MS-SO_3H/Pr, or MS-SO_3H/iBu, which contain ethyl, propyl, or isobutyl groups in the shell portion, were used. The adsorption of MF to the SO_3H-core/shell MMSS samples was improved by the incorporation of hydrophobic groups into the shell portion. These samples, which had higher catalytic activity, adsorbed larger amount of MF. Consequently, the concentration of the reactant in the mesopores could be elevated by introducing a hydrophobic shell layer to enhance the catalytic performance. However, in the case of MS-SO_3H/Ph, which contained bulky phenyl groups, the concentration of residual MF was 91%, and these particles adsorbed less MF. In addition, in the case of MS-SO_3H/Me, which contained less hydrophobic methyl groups, the adsorbed amount of MF was the same as that of MS-SO_3H/TMOS. In order to clarify the adsorption behavior of MF at 323 K at which the reactions were conducted, the adsorption test was performed at 323 K by changing the solvent from acetone to methanol. Even when the solvent was changed, the same tendency was observed with respect to the adsorption of MF.

3.3. Comparison with other types of MMSS catalysts

To investigate the importance of the core/shell structure, further tests were conducted on SO_3H-core/shell MMSS and other SO_3H functionalized MMSS samples. The samples that were compared were MS-SO_3H, MS-SO_3H-Et, and MS-SO_3H-Pr, which were synthesized by the co-condensation of TMOS and MPTMS (MS-SO_3H), TMOS, MPTMS and EtTMS (MS-SO_3H-Et), TMOS, MPTMS and PrTMS (MS-SO_3H-Pr), respectively. These samples were not core/shell particles and the organic functional groups were randomly distributed in the spherical particles. The molar fractions of MPTMS and EtTMS (or PrTMS) in the synthesis of MS-SO_3H-Et (-Pr) were 6.7 and 3.3 mol%, respectively, that were the same fractions in the core/shell MMSS. The properties of the samples are listed in Table 1 and the results of catalytic reactions are in Table 3. The catalytic activity of MS-SO_3H-Et and MS-SO_3H-Pr were higher than that of MS-SO_3H, indicating the effectiveness of the incorporation of hydrophobic groups. However, corresponding core/shell MMSS (MS-SO_3H/Et, MS-SO_3H/Pr) showed higher activity than MS-SO_3H-Et and Pr.

Examinations of the adsorption capabilities of the reactants (Table 4) showed that the core/shell MMSS adsorbed larger amounts of MF than MS-SO_3H-Et, which agreed with the above result and surely support that an appropriate core/shell structure enhances

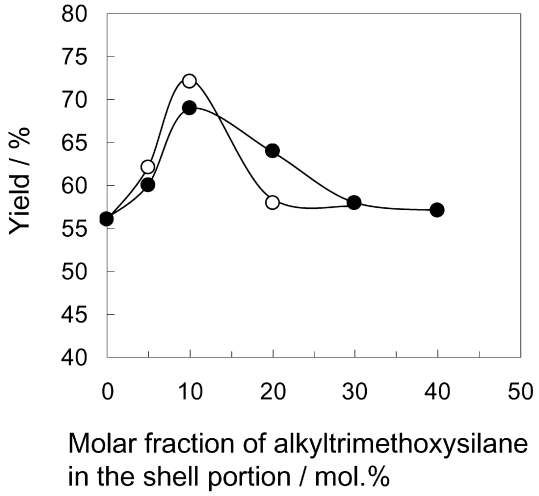

Fig. 11. Changes in the activity of MS-SO_3H/shell catalysts with various molar fractions of alkyl groups in condensation reaction for 2 h: (●) MS-SO_3H/Et, (○) MS-SO_3H/Pr.

catalytic performance. In the case of MS-SO_3H-Et, two organic functional groups (sulfonic acid and ethyl group) with different polar characters were randomly distributed in the particles. It is presumed that the presence of the polar sulfonic acid group close to the hydrophobic ethyl group slightly diminished the adsorption of hydrophobic MF on the ethyl group, and MS-SO_3H-Et adsorbed smaller amounts of MF than organically separately-functionalized core/shell MMSS (MS-SO_3H/Et).

When core/shell MMSS are used as catalysts, adsorption of the reactant happens in the shell portion. The reactant then moves to a catalytic site in the core portion, where the reaction proceeds. If the affinity of the shell layer for the reactant is too strong, diffusion of the reactant to the core portion is hindered, reducing the catalytic activity. It is believed that the affinity of ethyl or propyl groups in MS-SO_3H/Et or MS-SO_3H/Pr is appropriate for the reaction.

3.4. The effect of hydrophobic group ratio in the shell portion

In order to investigate the effect of hydrophobicity in the shell portion of SO_3H-core/hydrophobic-shell MMSS, MMSS having different molar fractions of ethyl or propyl groups in the shell portion were examined. The molar fractions of EtTMS or PrTMS incorporated were 5, 10, 20, 30, and 40 mol% (in case of ethyl groups), and the amount of additive silica source for shell portion was half that of the core portion. All the samples obtained were monodispersed and spherical, and the average particle diameters of the samples were almost the same (600 ± 30 nm). Fig. 11 shows the effect of the organic functional group molar fraction in the shell portion against the catalytic activity. When the molar fraction of EtTMS or PrTMS in the shell portion was 10 mol%, the yields were the highest (69 or 72%). The yields were decreased by reducing the number of organic functional groups in the shell portion, and in the case of MS-SO_3H/Et5% and MS-SO_3H/Pr5%, the yields were 60 and 62%. The hydrophobic reactant (MF) was considered to be a little difficult to enter into the shell portion, because the shell portion became less hydrophobic. On the other hand, increasing hydrophobicity in the shell portion by incorporating more hydrophobic groups also led to the decrease in the yield. The yield of MS-SO_3H/Et30% was as the same as that of MS-SO_3H which does not have a shell portion (58%). It is considered that the pore space in the shell portion became narrower by incorporating a lot of organic functional groups and the obstruction of the entry of reactants in the shell portion brought the decrease in the catalytic

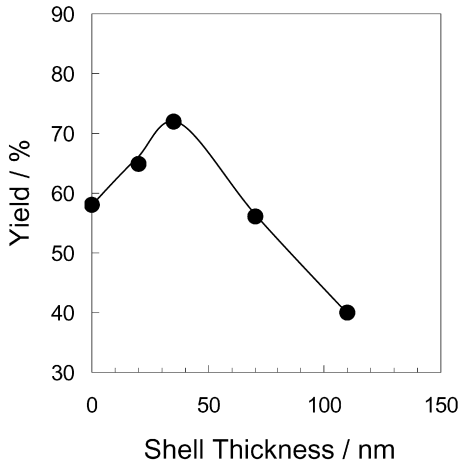

Fig. 12. Changes in the activity of MS-SO_3H/Pr catalysts with various shell thickness in condensation reaction for 2 h.

activity. In addition, the enhancement of hydrophobicity in the shell portion brought the decrease in the adsorbed amount of the other reactant (acetone), resulting in the decreased catalytic activity. In the case of propyl group that has larger molecular size than ethyl group, the yields decreased sharply to 58% by only 20 mol% of the incorporation (MS-SO_3H/Pr20%). When the molar fraction of propyl group increased to 20 from 10 mol%, the pore volume decreased from 0.67 to 0.62 ml/g. Consequently, it is thought that the reduction of the pore space in the shell portion would also result in the decrease in yield. It became clear that both the hydrophobicity and the pore space of the shell portion affect the catalytic activity of the core–shell MMSS. From the above results, it was found that the catalytic activity of the core–shell MMSS was the highest when the molar fraction of ethyl or propyl groups incorporated was 10 mol%, because of the well balanced hydrophobicity and the pore space.

3.5. The effect of the shell thickness of core/shell MMSS

Next, the effect of the shell thickness of the core/shell MMSS on the catalytic activity was examined using MS-SO_3H/Pr samples with different shell thicknesses. The molar fraction of PrTMS employed in these experiments was 10 mol%. Fig. 12 shows the effect of shell thickness on the catalytic activity. The yield was the highest when the shell thickness was 35 nm, and it became clear that optimum value existed in the shell thickness. When the shell layer was thinner than 35 nm, it is thought that it did not function well as hydrophobic site and the yields were lower. On the other hand, when the shell thickness became thicker than 35 nm, it is presumed that the entry of the reactant and the discharge of the product to and from the core portion were hindered because of longer distance between the catalytic core portion and the surface of the spherical particles. Consequently, it became clear that the thickness of the shell portion also affected the catalytic activity of the core/shell MMSS.

4. Conclusions

Organically functionalized core/shell MMSS containing sulfonic acid groups in the core portion and hydrophobic groups in the shell portion were successfully synthesized for the first time using the co-condensation/expansion method. These core/shell MMSS had well-ordered hexagonal mesopores, and it was confirmed from TEM observations that the compositions of the organic functional groups were clearly different in the core and the shell portions. It was shown that the acid catalytic activity of core/shell MMSS could be improved by changing the hydrophobicity and the thickness of the shell portion. The incorporation of ethyl or propyl groups in the shell layers led to high catalytic performance in the reaction. In addition, it was found that strong enhancements in catalytic activity due to the incorporation of hydrophobic groups were only achieved with core/shell structures; little enhancement was observed in randomly distributed structures. Thus, new types of selective catalysts and multi-step reaction catalysts can be synthesized by incorporating organic functional groups or metals into the core portion and/or the shell portion of core/shell MMSS.

References

[1] A.P. Wight, M.E. Davis, Chem. Rev. 102 (2002) 3589.
[2] F. Hoffmann, M. Cornelius, J. Morell, M. Fröba, Angew. Chem. Int. Ed. 45 (2006) 3216.
[3] J.A. Melero, R.V. Grieken, G. Morales, Chem. Rev. 106 (2006) 3790.
[4] W.M.V. Rhijn, D.E.D. Vos, B.F. Sels, W.D. Bossaert, P.A. Jacobs, Chem. Commun. (1998) 317.
[5] D. Das, J.F. Lee, S.F. Cheng, Chem. Commun. (2001) 2178.
[6] D. Das, J.F. Lee, S.F. Cheng, J. Catal. 223 (2004) 152.
[7] K. Wilson, A.F. Lee, D.J. Macquarrie, J.H. Clark, Appl. Catal. A 228 (2002) 127.
[8] K. Shimizu, E. Hayashi, T. Hatamachi, T. Kodama, T. Higuchi, A. Satsuma, Y. Kitayama, J. Catal. 231 (2005) 131.
[9] W.D. Bossaert, D.E.D. Vos, W.M.V. Rhijn, J. Bullen, P.J. Grobet, P.A. Jacobs, J. Catal. 182 (1999) 156.
[10] I. Díaz, F. Mohino, J. Pérez-Pariente, E. Sastre, Appl. Catal. A 205 (2001) 19.
[11] I. Díaz, C. Márquez-Alvarez, F. Mohino, J. Pérez-Pariente, E. Sastre, Microporous Mesoporous Mater. 44–45 (2001) 295.
[12] I.K. Mbaraka, D.R. Radu, V.S.Y. Lin, B.H. Shanks, J. Catal. 219 (2003) 329.
[13] S. Parambadath, M. Chidambaram, A.P. Singh, Catal. Today 97 (2004) 233.
[14] J.A. Melero, G.D. Stucky, R.V. Grieken, G. Morales, J. Mater. Chem. 12 (2002) 1664.
[15] J.A. Melero, R.V. Grieken, G. Morales, V. Nuno, Catal. Commun. 5 (2004) 131.
[16] X.G. Wang, C.C. Chen, S.Y. Chen, Y. Mou, S.F. Cheng, Appl. Catal. A 281 (2005) 47.
[17] B. Rac, A. Molnar, P. Forgo, M. Mohai, I. Bertoti, J. Mol. Catal. A Chem. 244 (2006) 46.
[18] M.A. Harmer, Q. Sun, M.J. Michalczyk, Z.Y. Yang, Chem. Commun. (1997) 1803.
[19] D.J. Macquarrie, S.J. Tavener, M.A. Harmer, Chem. Commun. (2005) 2363.
[20] M. Alvaro, A. Corma, D. Das, V. Fornes, H. Garcia, Chem. Commun. (2004) 956.
[21] D. Margolese, J.A. Melero, S.C. Christiansen, B.F. Chmelka, G.D. Stucky, Chem. Mater. 12 (2000) 2448.
[22] I. Díaz, C. Márquez-Alvarez, F. Mohino, J. Pérez-Pariente, E. Sastre, J. Catal. 193 (2000) 283.
[23] J. Pérez-Pariente, I. Díaz, F. Mohino, E. Sastre, Appl. Catal. A 254 (2003) 173.
[24] I. Díaz, C. Márquez-Alvarez, F. Mohino, J. Pérez-Pariente, E. Sastre, J. Catal. 193 (2000) 295.
[25] K. Yano, Y. Fukushima, Bull. Chem. Soc. Jpn. 75 (2002) 1977.
[26] K. Yano, Y. Fukushima, J. Mater. Chem. 13 (2003) 2577.
[27] K. Yano, Y. Fukushima, J. Mater. Chem. 14 (2004) 1579.
[28] T.M. Suzuki, M. Yamamoto, K. Fukumoto, Y. Akimoto, K. Yano, J. Catal. 251 (2007) 249.
[29] T.M. Suzuki, T. Nakamura, K. Fukumoto, M. Yamamoto, Y. Akimoto, K. Yano, J. Mol. Catal. A Chem. 280 (2008) 224.
[30] T.M. Suzuki, T. Nakamura, E. Sudo, Y. Akimoto, K. Yano, Microporous Mesoporous Mater. 111 (2008) 350.
[31] K. Yano, T. Nakamura, Chem. Lett. 35 (2006) 1014.
[32] T. Nakamura, M. Mizutani, H. Nozaki, N. Suzuki, K. Yano, J. Phys. Chem. C 111 (2007) 1093.
[33] J. Yang, Q.H. Yang, G. Wang, Z.C. Feng, J. Liu, J. Mol. Catal. A Chem. 256 (2006) 122.
[34] K. Inumaru, J. Kiyoto, S. Yamanaka, Chem. Commun. (2000) 903.